Entry of the bat influenza H17N10 virus into mammalian cells is enabled by the MHC class-II HLA-DR receptor

Efstathios S Giotis[1*], George Carnell[2 †], Erik F. Young[3 ††], Saleena Ghanny[3 †††], Patricia Soteropoulos[3 †††], Lin-Fa Wang[4], Wendy S Barclay[1], Michael A Skinner[1], Nigel Temperton[2]

[1]Section of Virology, Department of Medicine, St Mary's Campus, Imperial College London, UK.

[2]Viral Pseudotype Unit, Medway School of Pharmacy, University of Kent and University of Greenwich, Chatham Maritime, UK.

[3]Hackensack University Medical Center Department of Surgery, Hackensack, NJ.

[4]Programme in Emerging Infectious Disease, Duke-NUS Medical School, Singapore

Current affiliations:

[†]Laboratory of Viral Zoonotics, Department of Veterinary Medicine, University of Cambridge, UK.

[††]Bioelectronic Systems Lab, Columbia University, NY, USA.

[†††]Rutgers University, New Jersey Medical School Genomics Center, Newark, NJ, USA.

*Corresponding author: Efstathios S Giotis, e.giotis@imperial.ac.uk

Abstract

Haemagglutinin (HA) and neuraminidase (NA) surface glycoproteins of bat influenza H17N10 virus neither bind nor cleave sialic acid receptors, indicating this virus employs cell-entry mechanisms distinct from those of classical influenza A viruses. We observed that certain human haematopoietic cancer cell lines and the canine MDCK II cells are susceptible to H17-pseudotyped viruses. We identified the human HLA-DR receptor as an entry-mediator for H17-pseudotypes, suggesting that H17N10 possesses zoonotic potential.

Main

Bats are reservoirs of diverse, potentially zoonotic viruses (*e.g. Paramyxoviridae*, *Coronaviridae*, *Filoviridae)*, further exemplified by the discovery of the evolutionarily distinct, influenza A-like viruses H17N10 and H18N11 (BatIVs) in asymptomatic bats[1,2]. This discovery led to concern that bats may be neglected reservoirs of influenza viruses[3].

The natural reservoir of classical influenza A viruses (IAVs) is aquatic birds, from which they emerge, *via* genome reassortment and mutation, to cause sporadic pandemics in humans and other hosts[4]. The initial cross-species barrier is host cell attachment. The HA mediates virus binding to host-specific sialic acid (SA) moieties[4]. The crystal structures of BatIV HAs exhibit divergence of their protein conformations from those of IAVs and inability to accommodate SA[2,5,6]. Initial efforts to isolate infectious BatIVs from bats failed, mainly because their receptors were unknown[1,2,5,7,8]. Synthetic BatIVs were able to infect mammalian cell lines[9-11]. Identifying the BatIV receptors is key to assessing their zoonotic risk.

Lentivirus-derived pseudotypes (PV) with heterologous envelope proteins have facilitated identification of viral receptors[12] and are valuable in assessing H17N10 tropism[12,13]. We have shown that transduction-competent H17- and H17N10-PV are recovered from HEK293T/17 cells only in the presence of proteases (HAT or TMPRSS2) (Fig. 1a)[13], in keeping with published data[11]. To study the distribution of the H17N10 receptor(s), a panel of cell lines (Supplementary Table 1) was challenged with H17–PV, assaying transduction *via* the expression of PV-encoded luciferase reporter. PV bearing H5 (H5-PV) or VSV-G (VSV-G-PV) served as positive controls; PV without envelope protein (Δ-env) as negative. H17-PV displayed highly limited species/cell tropism, in agreement with previous work[9-11], suggesting the receptor(s) are not ubiquitous (Fig. 1b). Canine MDCK II (unlike MDCK I) cells are susceptible to H17-PV (Fig. 1c) in agreement with previous studies[10,11]. MDCK II cells were not susceptible to PV expressing N10 alone while particles bearing H17 alone or both H17 and

N10 transduced these cells with high, comparable efficiency, indicating that N10 is dispensable for entry, in keeping with published data[9,11]. To characterise the H17 putative receptor(s), MDCK II cells were (pre)-treated with enzymatic agents before transduction (Fig. 1d). Pre-treatment with neuraminidase, which cleaves surface SA, reduced transduction by H5-PV (by 68-86%) but not H17-PV, further supporting the notion that SA are not the H17-receptors[8-11].

IAVs primarily enter cells via endocytosis followed by low pH-triggered endosomal fusion. Treatment of cells with ammonium chloride blocked uptake of H5- and H17-PV, demonstrating that entry of H17, like IAVs, is pH-dependent consistent with a previous study[9]. Entry of H17-PV was more affected than H5-PV by pre-treatment of cells with proteases or an inhibitor of *N*-glycosylation (reduced by up to 72 and 78%, compared to 45 and 20%, respectively), supporting the supposition[9] that the H17-receptor(s) is a glycoprotein.

MDCK cells are heterogeneous, displaying phenotypic variation[14], with MDCK I and II representing early and late passages of the parental NBL-2 cells. Transcriptional differences between early (passage 8) and late (passage 21) MDCKs were investigated using microarrays, identifying 17 differentially regulated transcripts (Fig. 2a). Using transmembrane domain and subcellular localisation prediction algorithms, we identified the dog leukocyte antigen DRα-chain (DLA-DRA) as the only transcript encoding a surface-anchored protein, over-expressed in late, compared to early, passage cells (Supplementary Table 2). Significant over-expression of DLA-DRA (and paralogue DLA-DRB1) was confirmed by qRT-PCR in MDCK II compared to I cells (Fig. 2b).

DLA-DRA is a well-conserved orthologue of the human MHC-II HLA-DRA (Supplementary Figure 1). MHC-II molecules are heterodimers of two glycosylated, transmembrane polypeptide chains (monomorphic α and polymorphic β), expressed selectively on antigen presenting cells (APCs; Fig. 2c). HLA-DR forms complexes, with endocytosed foreign peptides, which are presented to $CD4^+$ T-helper cells for recognition[15].

To assess the zoonotic potential of H17N10, we explored the H17-PV tropism using human cell lines with known elevated HLA-DR expression levels[15] (Fig. 2d). Burkitt's lymphoma-derived Raji, Ramos and BJAB B-lymphocytes and the B-lymphoblastoid cells (B-LCL) show decreasing susceptibility, in that order, to H17-PV. Kasumi-1 leukaemic cells showed marginal susceptibility, while Molt-4 and HL-60 leukaemic cells, Jurkat T-cells, pro-monocytic THP-1 and U-937, and primary B-cells showed no susceptibility to H17-PV. Differential susceptibility to H17-PV correlated with HLA-DRA expression levels (confirmed by qRT-PCR). Surface expression of the heterodimer was assayed by flow cytometry (Fig. 2e)[16] and showed an association with susceptibility to H17-PV.

We investigated whether ectopic expression of HLA-DR was sufficient to render non-APC susceptible to H17-PV. HEK293T/17 cells were transiently co-transfected with the DRA and DRB1 expression vectors. Surface expression of the heterodimer was confirmed *via* immunofluorescence (Supplementary Figure 2). Flow cytometry confirmed 47% of cells formed a functional surface heterodimer (Fig. 2f). Over-expression of HLA-DR resulted in significant transduction by H17-PV. Furthermore, transduction was enhanced two-fold (Fig. 2g) in cells FACS-enriched for HLA-DR. Similar results were obtained using bat cells (Supplementary Figure 3). Conversely, small interfering RNA targeting HLA-DRA (Fig. 2h) or MHC-II monoclonal antibodies (Fig. 2i; Supplementary Figure 4) drastically reduced Raji cells' susceptibility to H17-PV.

Together, these findings demonstrate HLA-DR functions as a *bona fide* entry mediator for H17N10. Similarly, Karakus *et al* determined that bat, pig, mouse or chicken HLA-DR orthologues mediate cell entry of H18N11[17]. Through efficient binding to HLA-DR, BatIVs might simultaneously access APCs and block T-cell responses. This might explain the viruses' survival and asymptomatic status in carrier bats.

With limited functional information available on bat MHC-II, its role in the pathogenesis and transmission of BatIVs remains obscure. Nevertheless, the observation that H17N10 can enter human HLA-DR$^+$ cells implies that the virus has zoonotic potential.

Methods

Cell culture and treatment

Cell lines are described in Supplementary Table 1 and were cultured according to standard protocols (www.atcc.org). Bat cell lines were propagated in DMEM supplemented with heat-inactivated 15% fetal bovine serum (Life Technologies), penicillin (100 U/ml) and streptomycin (100 µg/ml; Invitrogen) and maintained at 37°C and 5% CO_2.

MDCK II cells were treated as previously[9] with either the endosomal acidification reagent ammonium chloride (1-100 mM), or pre-treated with neuraminidase from *Clostridium perfrigens* for 2 h (1-100 mM) or pronase for 30 min (endo- and exoproteases from *Streptomyces griseus* at 5-50 µg/ml; Calbiochem), or an *N*-glycosylation inhibitor for 5 h (tunicamycin at 0.01-1 µg/ml; Sigma-Aldrich). For experiments using glycosidases, Raji and Ramos cells were treated as previously[18] with 0-100 U/ml Peptide:*N*-glycosidase F (PNGase F; Calbiochem) or endoglycosidase H (endo H; New England Biolabs) or a mixture of neuraminidase (50 mM) and *O*-glycosidase (1-20 mU/ml) in Hank's Balanced Salt Solution (HBSS; Sigma) for 2 h at 37°C. Cells were washed twice with HBSS and transduced with H17- and VSV-G-PV for 2 h. The cells were then resuspended in fresh growth

medium for 24-48 h before assay. Bafilomycin A1 (Calbiochem) was used at a concentration of 10 nM. Cell viabilities were assessed by a trypan blue exclusion test.

Pseudotype production and susceptibility assays

Pseudotypes expressing H17 and N10 (from A/little yellow-shouldered bat/Guatemala/060/2011), H5 (A/Vietnam/1194/2004; H5N1 clade 1) or VSV (Vesicular Stomatitis Virus)-G glycoproteins were produced as described[13]. Briefly, the lentiviral packaging plasmid p8.91, the pCSFLW firefly luciferase vector, the pI.18 expression plasmids for H17 and/or N10 and the protease encoding plasmid pCAGGS-HAT were co-transfected using polyethylenimine (PEI) reagent (Sigma-Aldrich) into HEK293T/17 cells. Filtered supernatants were collected 48-72 h post transfection. To remove viral titer bias between different stocks, PV were concentrated and (re-) titrated by serial dilution. Concentration was carried out by ultra-centrifugation for 2 h at 25,000 rpm at 4°C (Beckman Optima XL-100 K Ultracentrifuge).

Two-fold serial dilutions of PV-containing supernatant were performed as previously described[13] using 96-well plates. Subsequently, $1x10^4$ (for adherent) and $3x10^4$ cells (for suspension) cells were added in 50 µl of medium per well. Plates were incubated for 24-48 h, after which 50 µl of Bright-Glo™ substrate (Promega) was added. Luciferase readings were conducted with a luminometer (FLUOstar OPTIMA, BMG Labtech) after a 5-min incubation. Data was normalized using Δ–env and cell-only measurements and expressed as Relative Luminescence Units (RLU)/ml.

Plasmids and transfections

Expression plasmids for HLA-DRA (NM_019111) and HLA-DRB1 (NM_001243965) were purchased from GenScript. HEK293T/17 at sub-confluence in 6-well plates or 100 mm dishes were transfected with HLA-DRA or HLA-DRB1 plasmids or a 1:1 combination of both

using Lipofectamine 3000 (Thermo Fisher). 48 h after transfection, cells were used either for immunofluorescence analysis, for FACS analysis or for PV-transduction. The transfection efficiency, as assessed by the GFP expression of a control plasmid, was >70% under microscopic observation. PakiTO3 cells were transfected with HLA-DR plasmids and selected with geneticin (500 µg/ml).

Microarray analysis

Total RNA was isolated from triplicates of early and late passage MDCK cells using a Ribopure kit (Ambion). Preparation of samples and hybridization to Affymetrix Canine Genome 2.0 GeneChips was performed according to standard Affymetrix protocols. A one-way ANOVA adjusted with the Benjamini–Hochberg multiple-testing correction (p<0.05) was performed with Partek Genomics Suite (v6.6) as previously described[19].

HLA-DRA knockdown and blocking using siRNA and monoclonal antibodies

A Sigma-Aldrich MISSION endonuclease-derived esiRNA (EHU226621) was used to knock down HLA-DRA expression in Raji cells. Lipofectamine RNAiMAX reagent (Thermo Fisher) was used to transfect exponentially grown cells with 50 nM of siHLA-DRA or of siControl (SIC001). Initial transfection was followed by re-transfection of cells on the following day. Cells were collected after 48 h and either seeded for transduction with PV or processed in order to validate siRNA activity (by qRT-PCR and western blot).

To evaluate the interaction of HLA-DR with H17, we used the broadly reactive MHC-II mAb WR18 (Biorad; code MCA477) and anti-HLA-DR mAb (clone 302CT2, Enzo Life Sciences). After 1 h pre-incubation with increasing mAb concentrations of the antibody, Raji cells ($3x10^4$) were transduced for 2 h with H17-or VSV-G-PV. The cells were then resuspended in fresh growth medium and luciferase was measured after 24 h.

Western blot analysis

Washed cells were lysed on ice with lysis buffer [0.5% NP40 in PBS with 10 mM Tris-HCl, pH 7.4 supplemented with protease inhibitors (Thermo Fisher)] and protein was quantified by the BCA assay kit (Thermo Fisher). 20-50 μg of protein was electrophoresed on a 4-15% sodium dodecylsulfate polyacrylamide gel, alongside a protein ladder (Bio-Rad) and immunoblotted with the mouse mAb anti-HLA-DRA (1:1000; clone: 302CT2, Enzo Life Sciences) or rabbit mAb a-tubulin (1:2000; Cell signalling Technology). The membranes were washed and incubated with goat anti-rabbit or donkey anti-mouse secondary antibodies (LI-COR) in the dark for 1 h. Scanning was carried out using the Odyssey Imaging system.

Immunofluorescence

Transfected cells were seeded onto glass cover slips overnight and were fixed with 4% paraformaldehyde. Fixed cells were then washed and permeabilised with 1% Triton X-100 in PBS for 10 minutes. After washing, the cover slips were incubated with a mouse HLA-DRA mAb (169-1B5.2; Bio-Techne) targeting a monomorphic HLA-DR framework determinant for 1 hr, washed and incubated with anti-mouse Alexafluor488 conjugated-Ab (Thermo Fisher) for 30 minutes. Cover slips were mounted using Prolong Gold containing DAPI (Invitrogen). Images were acquired on EVOS fluorescent microscope (Life Technology). Experiments were carried out in duplicate.

Flow cytometry

For surface staining, cells were washed twice in ice-cold FACS buffer and stained with a FITC-conjugated anti-human HLA-DR mAb (clone Tü36; BDIS), which binds to a monomorphic epitope of the αβ complex and not the isolated α or β chains or the HLA-DP and -DQ isotypes[16]. The BD LSR Fortressa was used to determine expression of HLA-DR, in combination with the matched isotype control and cells were sorted into HLA-DR$^-$ and HLA-

207 DR^+ subpopulations with a FACS Aria cell sorter (BDIS). The Hoechst 33342 stain was used for
208 cell viability discrimination and the data files were analyzed using FlowJo software v10.0
209 (Tree Star, Inc.). Experiments were carried out in duplicate. Gating strategy: cells were first
210 identified by forward (FSC-Area) versus side scatter (SSC-Area) gating based on cell size and
211 granularity, then the FSC-Area vs FSC-Height gating for single cells. Dead cells were excluded
212 by gating on Hoechst 3342 negative cells. Positive and negative gates for HLA-DR expression
213 were determined by using isotype and unstained controls.
214
215 **qRT-PCR analysis**
216 qRT-PCR was performed using procedures described previously[19]. qRT-PCR was conducted in
217 a 384-well plate with the ABI-7900HT system (Applied Biosystems). The following primers
218 were used: DLA-DRA (Forward: 5'-GCTGTGGACAAAGCTAACCTTG-3', Reverse: 5'-
219 TCTGGAGGTACATTGGTGTTCG-3'), DLA-DRB1 (Forward: 5'-AGCACCAAGTTTGACAAGC-3',
220 Reverse: 5-AAGAGCAGACCCAGGACAAAG-3'). Absolute copy numbers of HLA-DRA were
221 calculated using a standard curve of known concentrations of the corresponding expression
222 plasmid. HLA-DRA (Forward: 5'-TCAAGGGATTGCGCAAAAGC-3', Reverse: 5'-
223 ACACCATCACCTCCATGTGC-3').
224
225 **Bioinformatic and statistical analyses**
226 Phobius[20] and TMHMM v2.0[21] software were used to predict the existence of transmembrane
227 domains and Deeploc-1.0[22] was used to determine sub-cellular protein localisation. The
228 amino acid sequences of DLA-DRA (NP_001011723.1), HLA-DRA (NP_061984.2), and their bat
229 orthologues [(*Pteropus alecto* (XP_006907484.1); *Desmodus rotundus* (XP_024413747.1)]
230 were subjected to multiple alignment using CLC workbench 7. Graphical representation and
231 statistical analyses were performed using Prism 8 (GraphPad). Unless otherwise stated,
232 results are shown as means ± SEM from three independent experiments. Selection of

statistical analysis was based on the data distribution. Data distributions were tested for normality using the Shapiro–Wilk normality test. $p<0.05$ was considered significant unless otherwise stated.

Ethics statement: The buffy coat residues for the isolation of $CD19^+$ primary B-cells were purchased from the UK Blood Transfusion Service from anonymous volunteer blood donors. Therefore, no ethical approval is required.

Competing Interests

The authors declare no competing interests.

Data Accessibility

Microarray data are available at the GEO repository under series record number GSE14837. All other data supporting the findings of this study are available from the authors on request.

References:

1. Tong, S. *et al. Proc. Natl Acad. Sci. USA* **109**, 4269-4274 (2012).
2. Tong, S. *et al. PLoS Pathog* **9**, e1003657 (2013).
3. Ciminski, K. *et al. J. Gen. Virol.* **98**, 2393-2400 (2017).
4. Long, J. S. *et al. Nat. Rev. Microbiol.* (2018).
5. Sun, X. *et al. Cell Rep.* **3**, 769-778 (2013).
6. Zhu, X. *et al. Proc. Natl Acad. Sci. U S A* **109**, 18903-18908 (2012).
7. Juozapaitis, M. *et al. Nat. Commun.* **5**, 4448 (2014).
8. Wu, Y. *et al. Trends Microbiol.* **22**, 183-191 (2014).
9. Maruyama, J. *et al. Virology* **488**, 43-50 (2016).
10. Moreira, E. A. *et al. Proc. Natl Acad. Sci. USA* **113**, 12797-12802 (2016).
11. Hoffmann, M. *et al. PLoS ONE* **11**, e0152134 (2016).
12. Carnell, G. W. *et al. Front. Immunol.* **6**, 161 (2015).
13. Carnell, G. *et al. Biorxiv*, doi:http://dx.doi.org/10.1101/499947. (2018).
14. Dukes, J. D. *et al. BMC Cell Biol.* **12**, 43 (2011).
15. Roche, P. A. *et al. Nat. Rev. Immunol.* **15**, 203-216 (2015).
16. Ziegler, A. *et al. Immunobiology* **171**, 77-92 (1986).
17. Karakus, U. *et al. Nature* **567**, 109-112 (2019).

18. de Vries, E. *et al. Proc. Natl Acad. Sci. USA* **109**, 7457-7462 (2012).
19. Giotis, E. S. *et al. Sci. Rep.* **7**, 17485 (2017).
20. Kall, L. *et al. Nucleic Acids Res.* **35**, W429-432 (2007).
21. Krogh, A. *et al. J. Mol. Biol.* **305**, 567-580 (2001).
22. Almagro-Armenteros, J. J. *et al. Bioinformatics* **33**, 4049 (2017).

Figure Legends

Figure 1: a. PV-production schematic. **b.** H17-PV transduction efficiencies in cell lines (*n*=6). Relative Luminescence Units (RLU)/ml are plotted as box-plots (Upper/lower bounds: 25% and 75% quantiles; middle band: median; whiskers: minimum-maximum values). **c.** PV-transduction efficiencies (means ± SEM, *n*=8) in MDCK II cells. Statistical significance was determined by Kruscal-Wallis and Dunn's *post-hoc* tests. **d.** Left Y-axis: % PV-transduction efficiencies in (pre-)treated MDCK II cells (means ± SEM, *n*=4). Right Y-axis: % cell viability (means ± SEM, *n*=3).

Figure 2: a. Up-/down-regulated (green/red) transcripts identified by microarrays in late- versus early-passaged MDCKs. Red box: membrane protein-encoded transcript. **b.** mRNA expression levels (means ± SEM, *n*=4) of DLA-DRA/-DRB1. Significance was calculated by one-way ANOVA and Tukey's tests (***p=0.0006; ****p<0.0001). **c.** HLA-DR schematic (Motifolio). **d.** Left Y-axis: H17-PV transduction efficiencies in human cell lines [*n*=4; box-plot (top/bottom: min/max values; middle band: median)]. Right Y-axis (line): HLA-DRA mRNA copies (*n*=4). **e.** FACS analysis of HLA-DR cell surface expression (representative of two independent experiments). Blue and red peaks represent HLA-DR$^-$ and -DR$^+$ subpopulations. **f.** FACS analysis of HLA-DR expression in HEK293T/17 cells transfected with HLA-DRαβ plasmids (*n*=2)**.** Right top corner: immunofluorescence confirming HLA-DR expression (*n*=2; Scale bar=10 μm). **g.** PV-transduction efficiencies (means ± SEM, *n*=4) in FACS-sorted DR$^-$, unsorted (DR$^+$ & DR$^-$) and FACS-sorted DR$^+$ HEK293T/17 cells. Significance was calculated by one-way ANOVA and Tukey's tests (****p<0.0001). **h.** Left: PV-transduction efficiencies (means ± SD, *n*=3) in Raji cells transfected with siControl or siHLA-DRA. Significance was

calculated with a *t*-test (Holm-Sidak-adjusted) and right: corresponding western blot and qRT-PCR data showing HLA-DRA protein and mRNA levels (means ± SD, *n*=3). qRT-PCR significance was calculated by two-sided *t*-test (*p*=0.0065). **i.** % PV-transduction levels (means ± SD, *n*=3) in Raji cells pre-incubated with MHC-II monoclonal antibody. Significance was calculated by one-way ANOVA and Dunnett's tests (***p=0.0003, ****p<0.0001).

Corresponding author

Correspondence and requests for materials to Efstathios S Giotis

Acknowledgements:

Our thanks go to Jim Kaufman, Yanping Guo, Ibrahim Elbusifi, Daragh Quinn, Alfred Ho, Kevin Ciminski and Martin Schwemmle for their support. Cells were kindly provided by Dr Edward Wright (University of Sussex, UK), Dr Konstantinos Paschos, Dr Rob White, Dr Marcus Dorner, Dr Michael Edwards, Professor Paul Farrell and Professor Robin Shattock (Imperial College London). This research was undertaken with the financial support of the Biotechnology and Biological Sciences Research Council (BBSRC) (http://www.bbsrc.ac.uk) via Strategic LoLa grant BB/K002465/1 "Developing Rapid Responses to Emerging Virus Infections of Poultry (DRREVIP)" and the Octoberwoman Foundation. L-FW is supported by the Singapore National Research Foundation grants (NRF2012NRF-CRP001-056 and NRF2016NRF-NSFC002-013).

Author Contributions: ESG conceived, designed and performed the experiments, analysed data and wrote the manuscript. GC generated luciferase reporter plasmids, produced pseudotype viral stocks and wrote the manuscript. EFY, SG and PS performed microarray work. WSB, MAS, and NT designed experiments and wrote the manuscript. L-FW provided materials and engaged in discussion of the project.

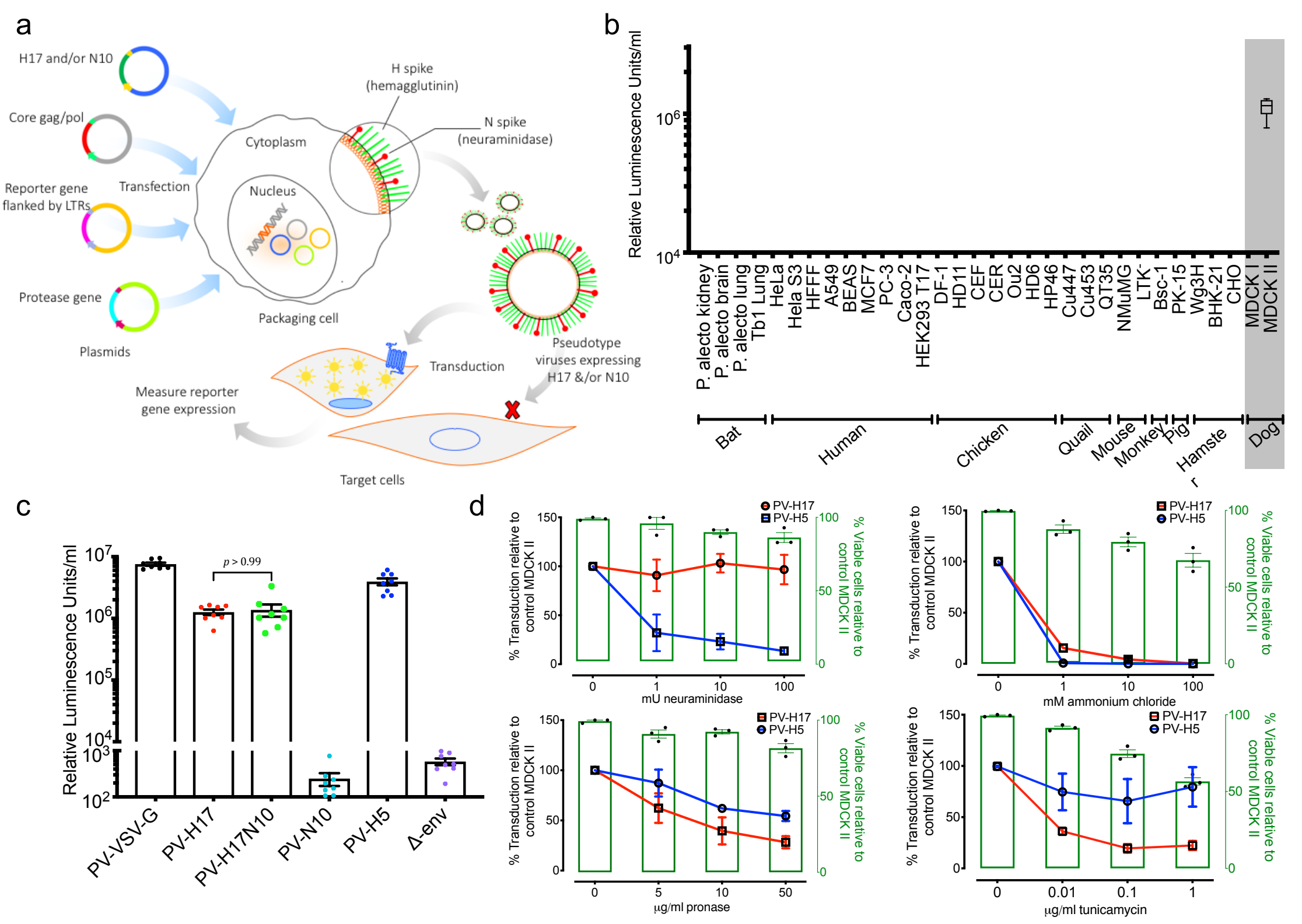
a
H17 and/or N10
Core gag/pol
Reporter gene flanked by LTRs
Protease gene
Plasmids
Transfection
Cytoplasm
Nucleus
Packaging cell
H spike (hemagglutinin)
N spike (neuraminidase)
Pseudotype viruses expressing H17 &/or N10
Transduction
Measure reporter gene expression
Target cells
b
Relative Luminescence Units/ml
10^6
10^4
P. alecto kidney
P. alecto brain
P. alecto lung
Tb1 Lung
HeLa
Hela S3
HFFF
A549
BEAS
MCF7
PC-3
Caco-2
HEK293 T17
DF-1
HD11
CEF
CER
Ou2
HD6
HP46
Cu447
Cu453
QT35
NMuMG
LTK-
Bsc-1
PK-15
Wg3H
BHK-21
CHO
MDCK I
MDCK II
Bat
Human
Chicken
Quail
Mouse
Monkey
Pig
Hamster
Dog
c
Relative Luminescence Units/ml
10^7
10^6
10^5
10^4
10^3
10^2
p > 0.99
PV-VSV-G
PV-H17
PV-H17N10
PV-N10
PV-H5
Δ-env
d
PV-H17
PV-H5
% Transduction relative to control MDCK II
% Viable cells relative to control MDCK II
mU neuraminidase
mM ammonium chloride
µg/ml pronase
µg/ml tunicamycin

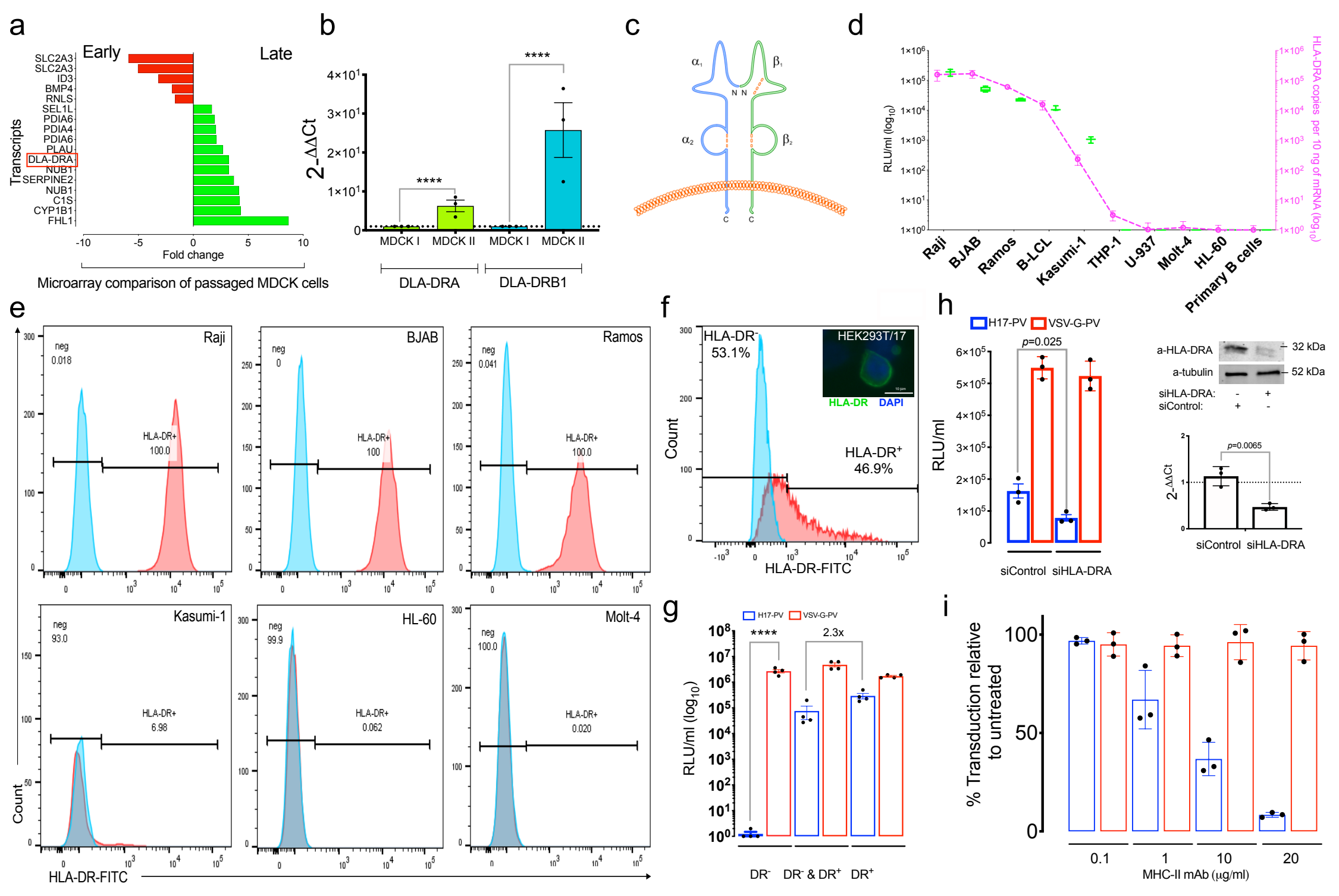
a
Early
Late
SLC2A3
SLC2A3
ID3
BMP4
RNLS
SEL1L
PDIA6
PDIA4
PDIA6
PLAU
DLA-DRA
NUB1
SERPINE2
NUB1
C1S
CYP1B1
FHL1
Transcripts
-10
-5
0
5
10
Fold change
Microarray comparison of passaged MDCK cells
b
2-ΔΔCt
****
****
MDCK I
MDCK II
MDCK I
MDCK II
DLA-DRA
DLA-DRB1
c
α1
β1
N N
α2
β2
C C
d
RLU/ml (log10)
HLA-DRA copies per 10 ng of mRNA (log10)
Raji
BJAB
Ramos
B-LCL
Kasumi-1
THP-1
U-937
Molt-4
HL-60
Primary B cells
e
Raji
neg
0.018
HLA-DR+
100.0
BJAB
neg
0
HLA-DR+
100
Ramos
neg
0.041
HLA-DR+
100.0
Kasumi-1
neg
93.0
HLA-DR+
6.98
HL-60
neg
99.9
HLA-DR+
0.062
Molt-4
neg
100.0
HLA-DR+
0.020
Count
HLA-DR-FITC
f
HLA-DR-
53.1%
HEK293T/17
HLA-DR
DAPI
HLA-DR+
46.9%
Count
HLA-DR-FITC
g
H17-PV
VSV-G-PV
****
2.3x
RLU/ml (log10)
DR-
DR- & DR+
DR+
h
H17-PV
VSV-G-PV
p=0.025
RLU/ml
siControl
siHLA-DRA
a-HLA-DRA
a-tubulin
32 kDa
52 kDa
siHLA-DRA:
siControl:
p=0.0065
2-ΔΔCt
siControl
siHLA-DRA
i
% Transduction relative to untreated
MHC-II mAb (μg/ml)
0.1
1
10
20

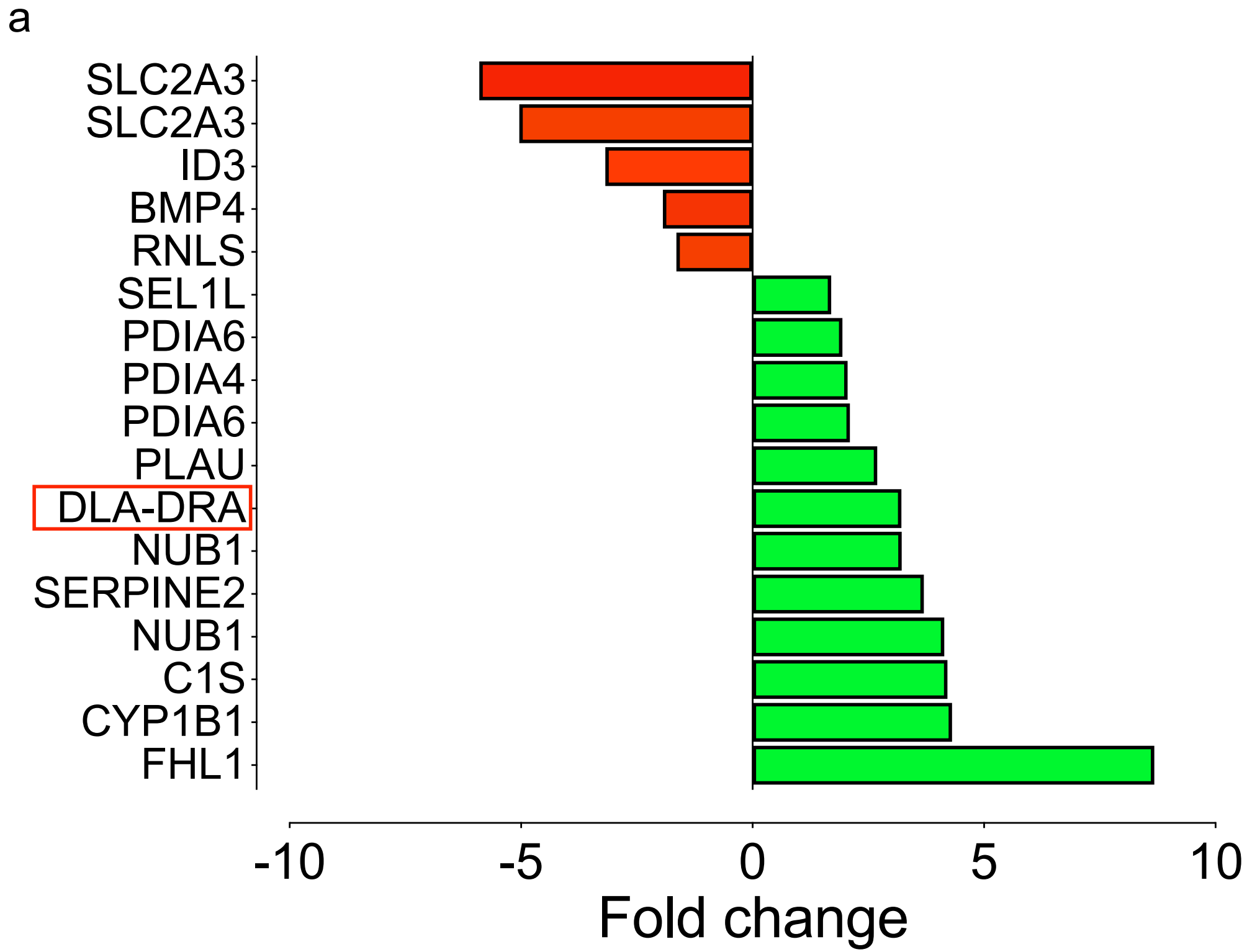
a
SLC2A3
SLC2A3
ID3
BMP4
RNLS
SEL1L
PDIA6
PDIA4
PDIA6
PLAU
DLA-DRA
NUB1
SERPINE2
NUB1
C1S
CYP1B1
FHL1
-10
-5
0
5
10
Fold change

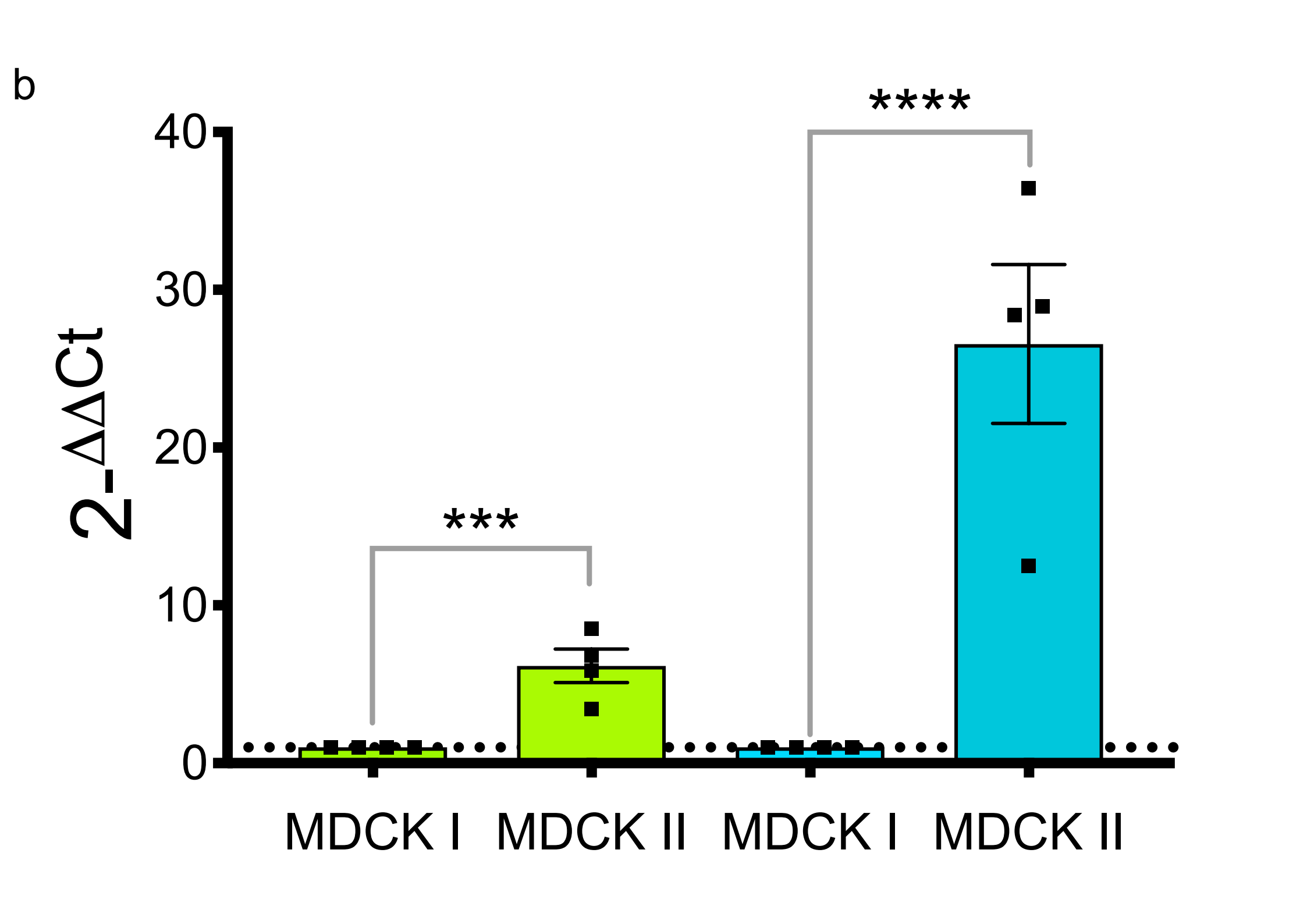
b
40
30
20
10
0
2-ΔΔCt
***
****
MDCK I
MDCK II
MDCK I
MDCK II

C

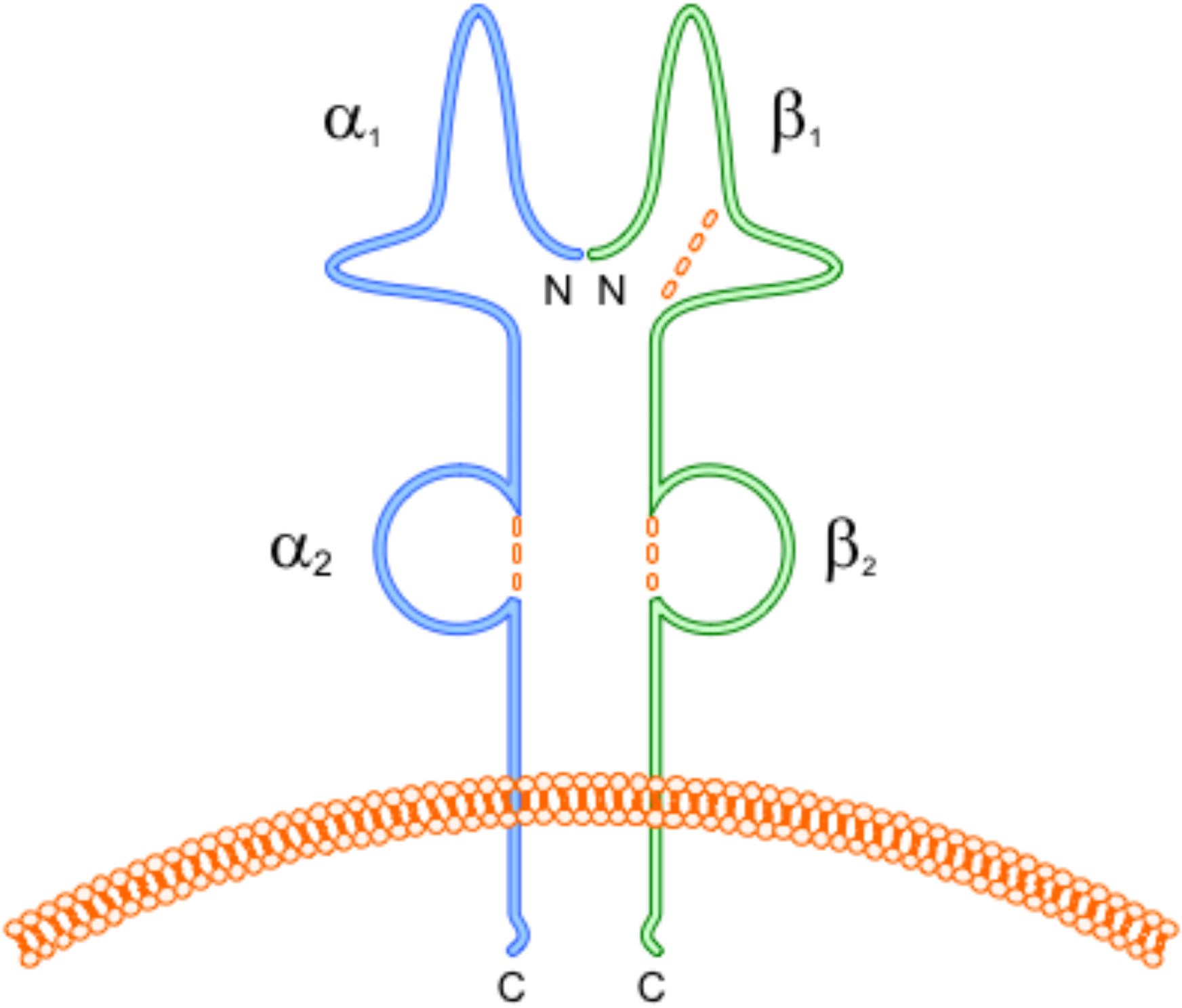

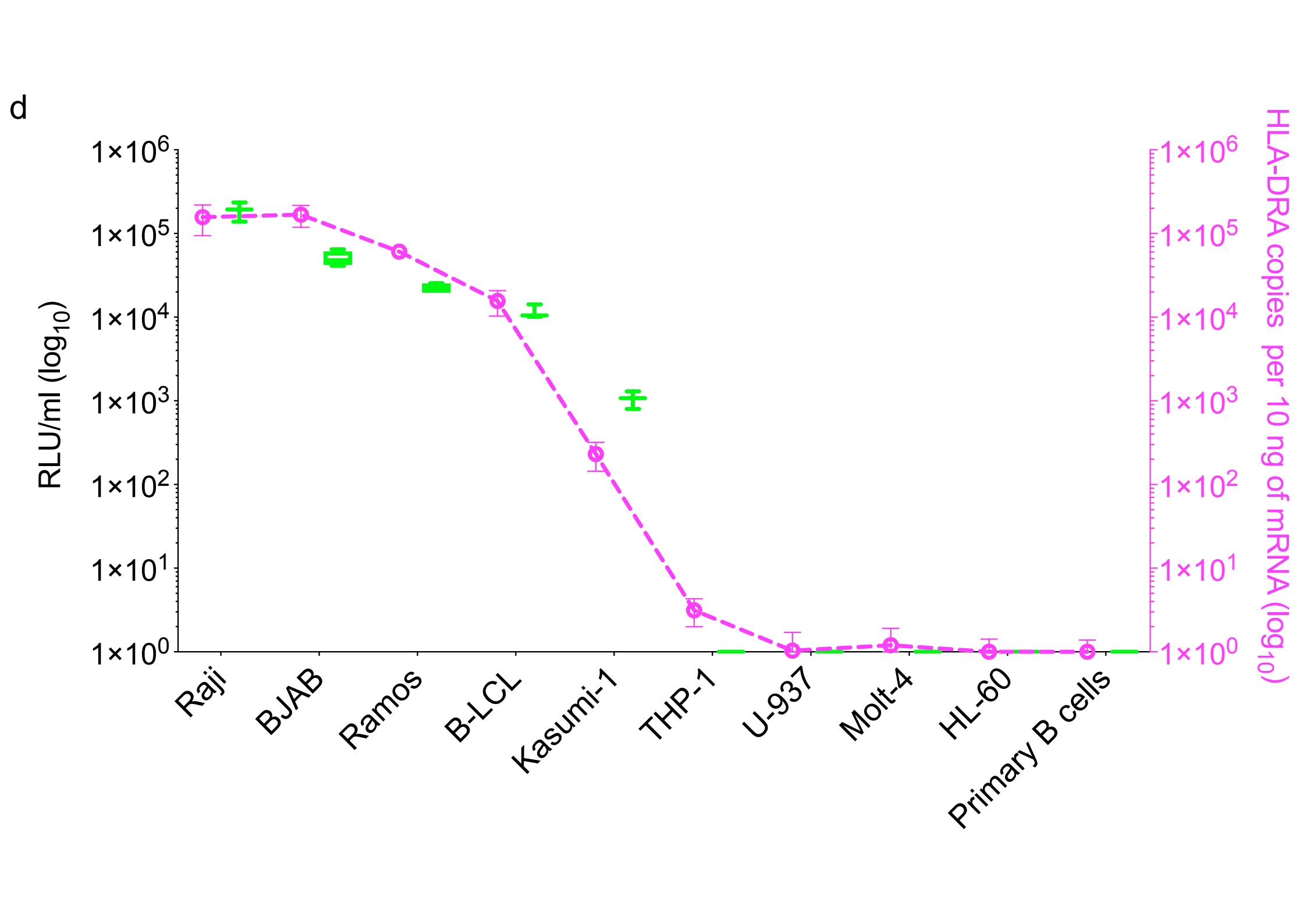
d
RLU/ml (log10)
HLA-DRA copies per 10 ng of mRNA (log10)
1×10^6
1×10^5
1×10^4
1×10^3
1×10^2
1×10^1
1×10^0
Raji
BJAB
Ramos
B-LCL
Kasumi-1
THP-1
U-937
Molt-4
HL-60
Primary B cells

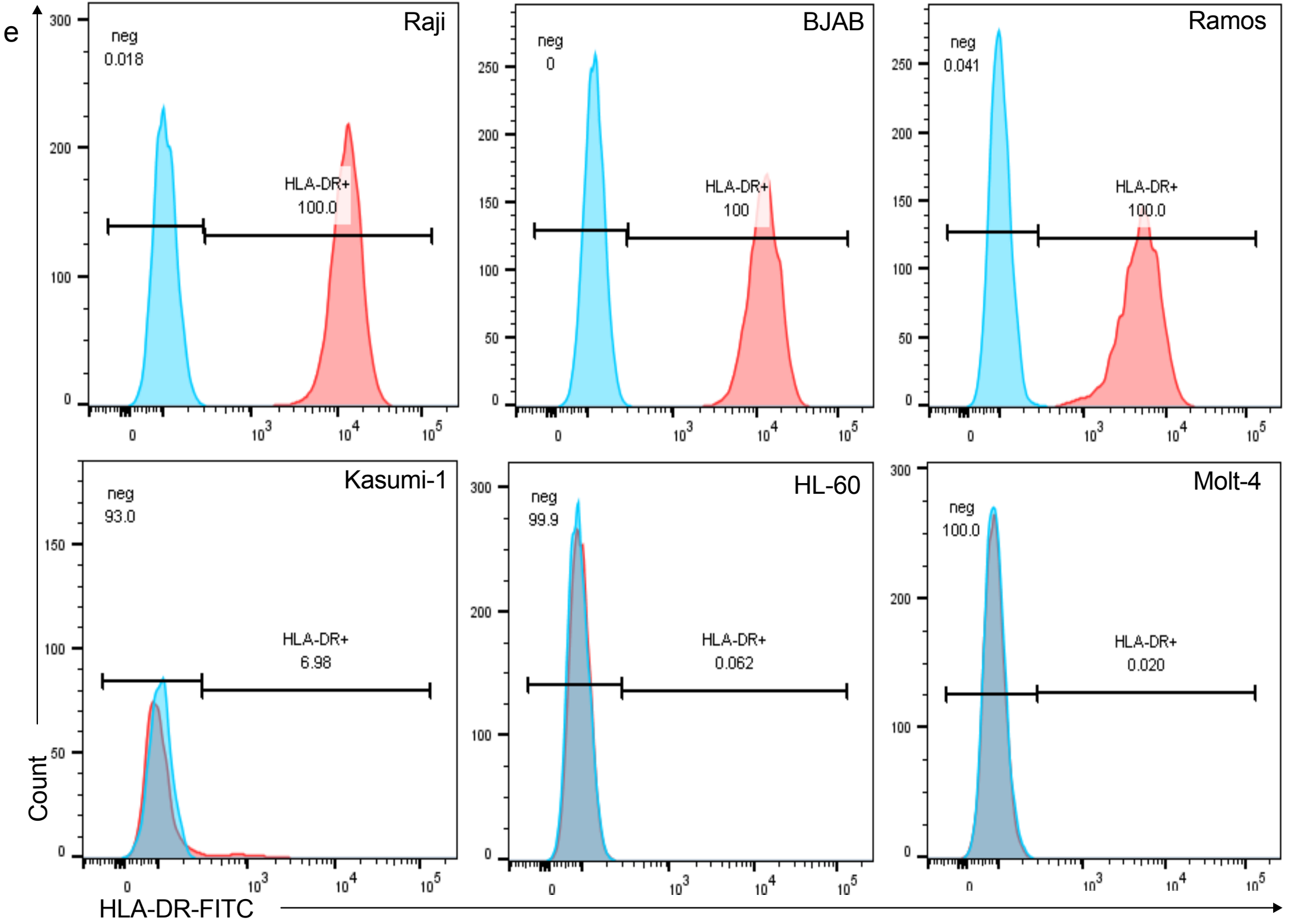
e
Raji
neg
0.018
HLA-DR+
100.0
BJAB
neg
0
HLA-DR+
100
Ramos
neg
0.041
HLA-DR+
100.0
Kasumi-1
neg
93.0
HLA-DR+
6.98
HL-60
neg
99.9
HLA-DR+
0.062
Molt-4
neg
100.0
HLA-DR+
0.020
Count
HLA-DR-FITC

f

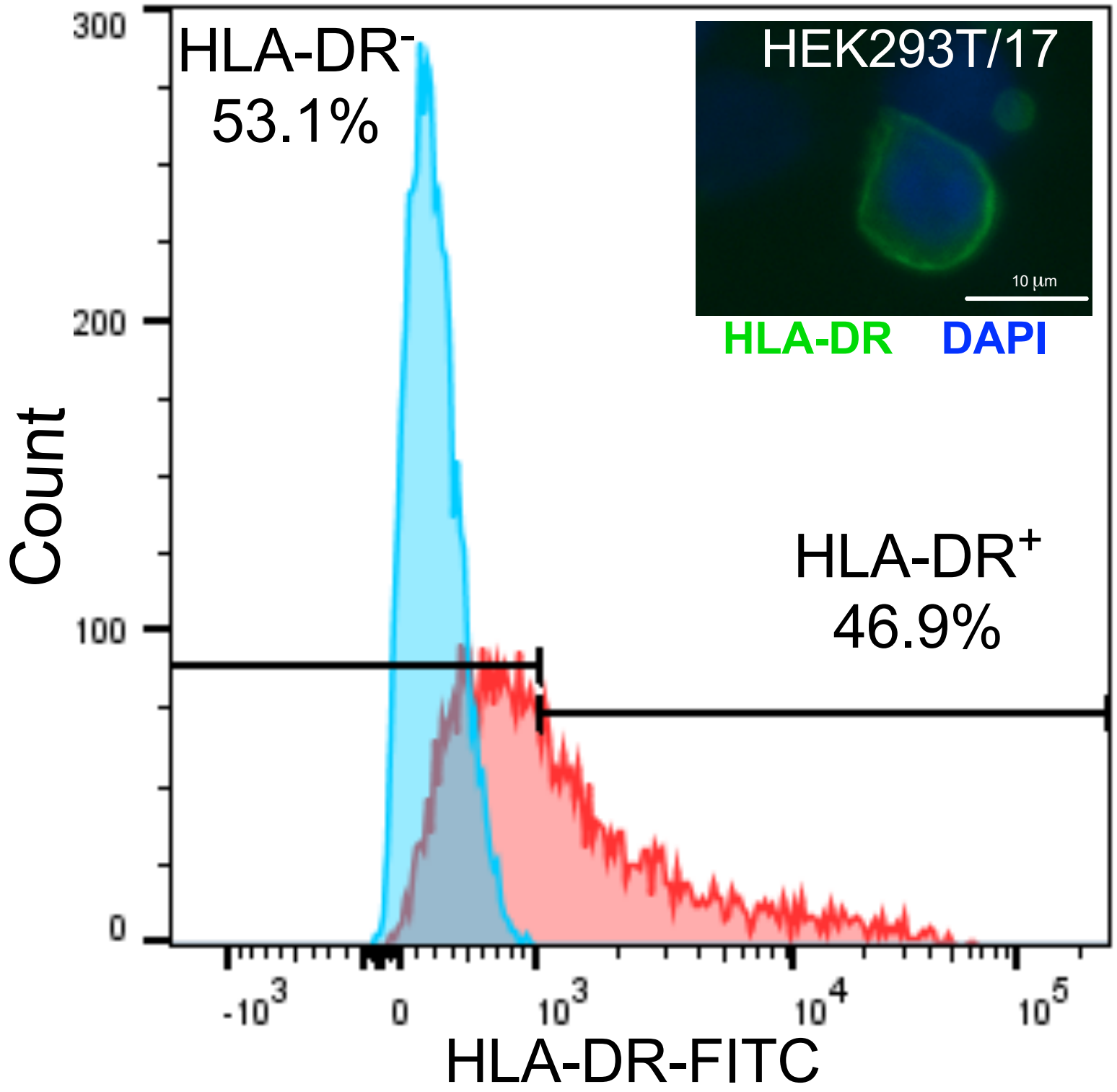
HLA-DR-
53.1%
HEK293T/17
10 µm
HLA-DR DAPI
HLA-DR+
46.9%
Count
300
200
100
0
-10^3
0
10^3
10^4
10^5
HLA-DR-FITC

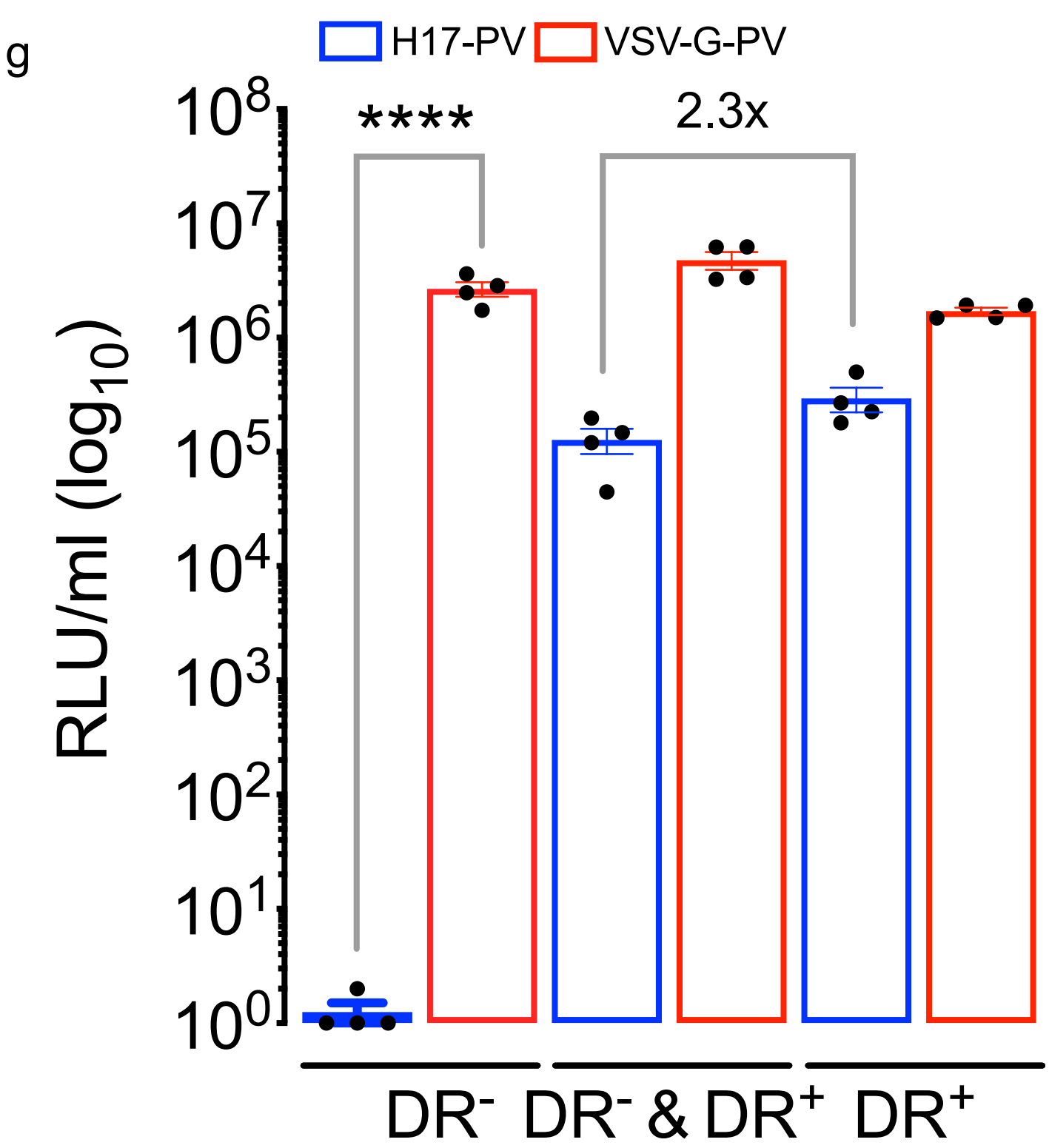
g
H17-PV
VSV-G-PV
****
2.3x
RLU/ml (log10)
10^8
10^7
10^6
10^5
10^4
10^3
10^2
10^1
10^0
DR-
DR- & DR+
DR+

h

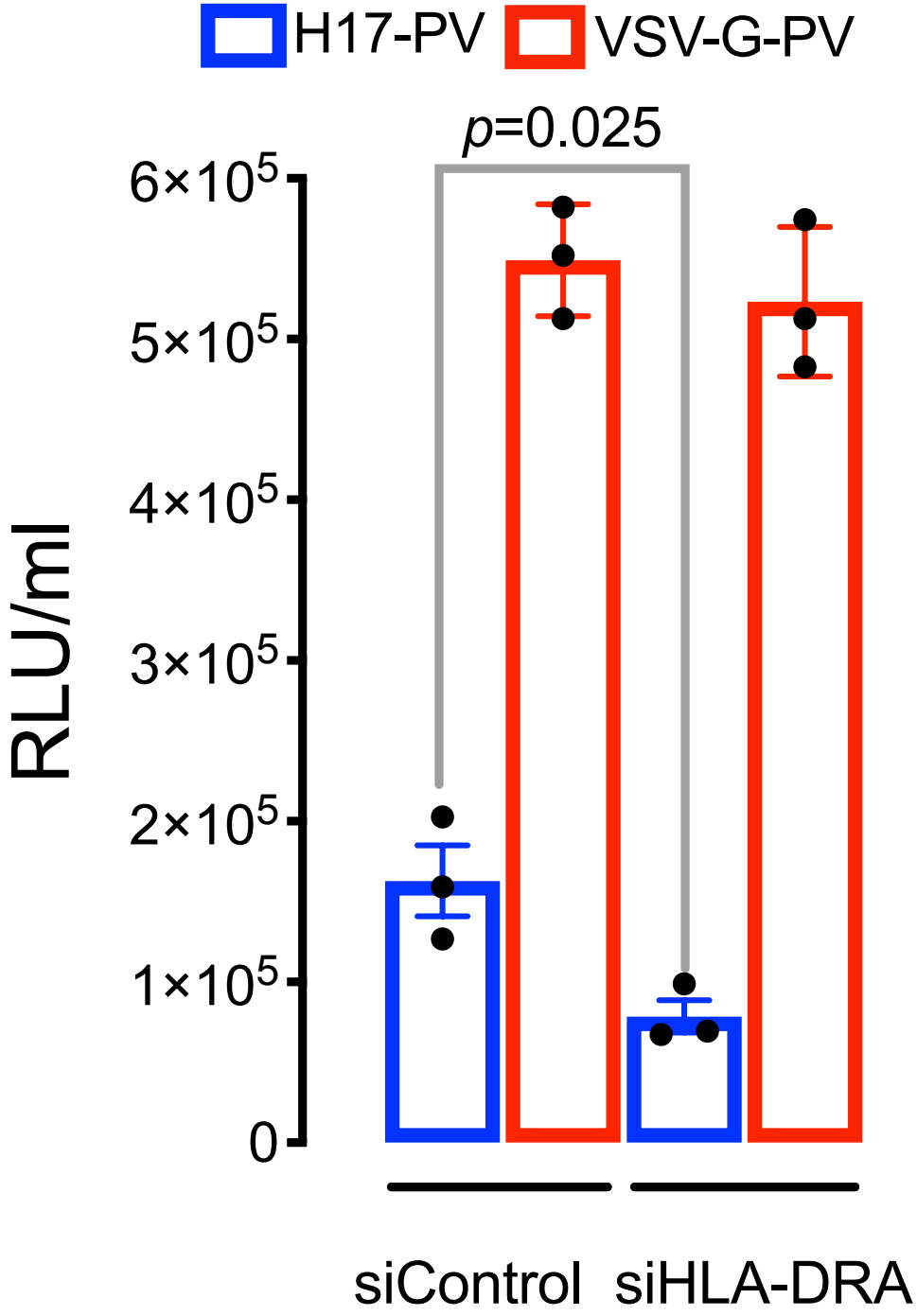
H17-PV
VSV-G-PV
p=0.025
RLU/ml
6×10^5
5×10^5
4×10^5
3×10^5
2×10^5
1×10^5
0
siControl
siHLA-DRA

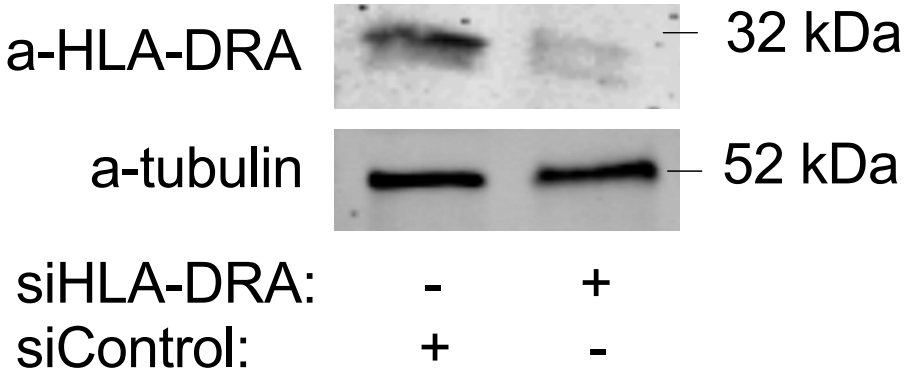
a-HLA-DRA
32 kDa
a-tubulin
52 kDa
siHLA-DRA: - +
siControl: + -

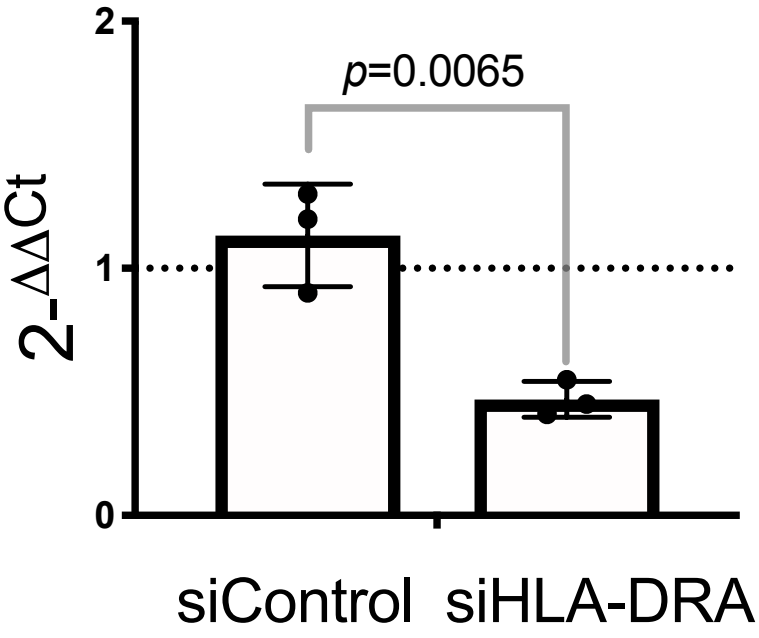
p=0.0065
2^-ΔΔCt
2
1
0
siControl
siHLA-DRA

i

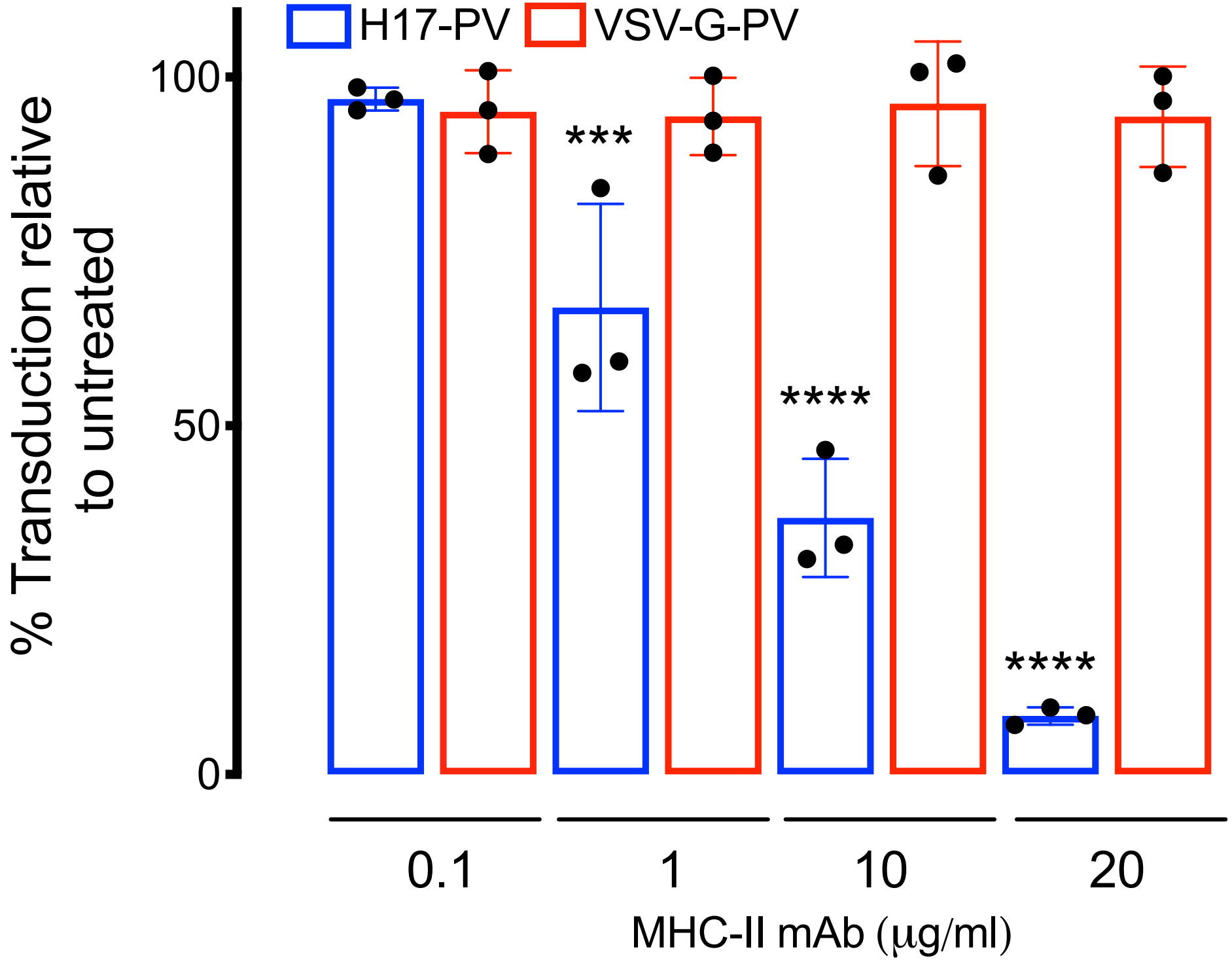
H17-PV
VSV-G-PV
% Transduction relative to untreated
100
50
0
***
****
****
0.1
1
10
20
MHC-II mAb (μg/ml)